Characterization of Lunar Thermal Environments: Regional and Terrain Effects on Sink Temperature

Presented by: Will Grier

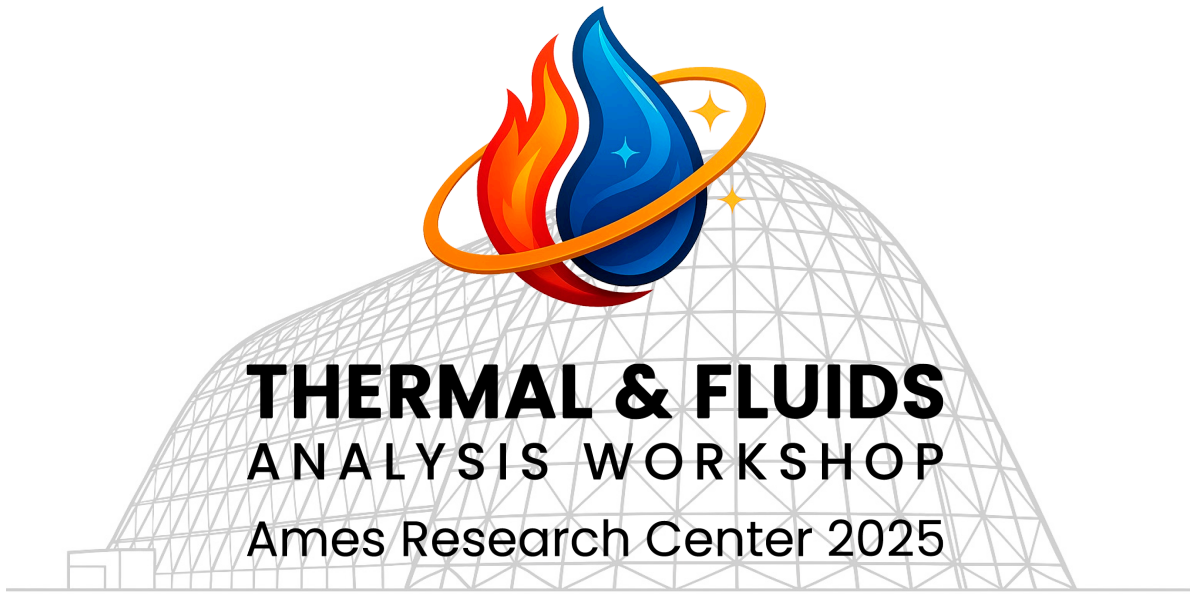

Will Grier (LaRC-D206), will.j.grier@nasa.gov
Lisa Erickson (JSC-EC611), lisa.erickson@nasa.gov
Will Birmingham (MSFC-EV34), william.j.birmingham@nasa.gov

Thermal & Fluids Analysis Workshop 2025
NASA Ames Research Center
San Jose, CA
August 4-7, 2025

Outline

- Study Purpose
- LUMENATE Overview
  - Description and Products
- Lunar Surface Thermal Environment
- Flux Cube Sink Temperature Method
- Simple Lunar Terrain Model
  - Methods and Results
- Detailed Lunar Terrain Model
  - Methods and Results
- Thermal Impacts of Dust Coverage
- Methods to Predict Lunar Surface Temperature
- Findings and Remarks
- References

Study Purpose

- Introduce the LUnar and Mars ENvironments Analysis Team (LUMENATE) and relevant products:
  - Thermal insights for NESC cold tolerant electronics for Lunar applications report
  - Detailed terrain modeling for Artemis III Human Landing System (HLS) extravehicular activities (EVAs)

- Investigate differences between Lunar surface temperatures and the environmental sink temperatures of a representative asset at various regional locations on the Lunar surface
  - Demonstrate using the flux cube method to gather sink temperatures across a range of optical properties
  - Use generated optical property ratio plots to infer thermal impacts from dust deposition on asset surfaces

- Compare Lunar surface temperature and environmental sink temperature predictions between thermal models using simple and detailed terrain models
  - Highlight discrepancies between simplified flat plane and detailed terrain models for South Pole regions where low solar elevation angles and terrain features significantly impact thermal conditions

LUnar and Mars ENvironments Analysis Team (LUMENATE)

The LUMENATE team delivers Lunar and Martian thermal environmental modeling expertise to NASA and industry:

- Develop guidance documentation and reference models for performing Lunar and Martian environmental thermal analysis
- Address environmental knowledge gaps identified during system development efforts and missions
- Create and improve advanced environmental thermal analysis techniques that support diverse missions and systems

Current duties include:

- Update the Lunar Thermal Analysis Guidebook (LTAG)[1]
- Develop a Mars Thermal Analysis Guidebook (MTAG)
- Develop novel thermal analysis capability for Artemis III and beyond surface missions to inform EVA planning

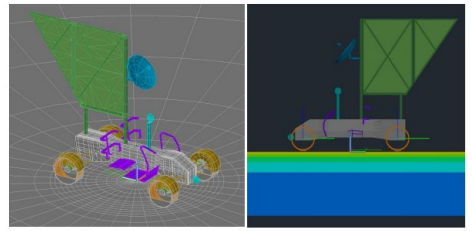

Thermal Sensitivity of LTV Wheels, Will Birmingham (MSFC-EV34)[3]

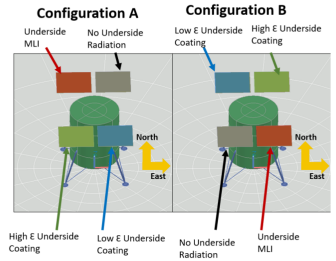

Lunar Latitude and Terrain Radiator Sensitivity, Will Birmingham (MSFC-EV34)[4]

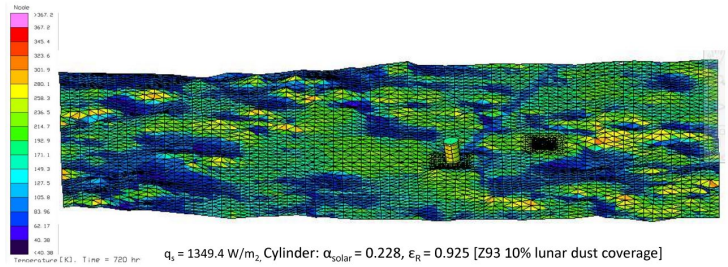

Lunar Surface 3D Terrain Modeling, Lisa Erickson (JSC-EC611)[2]

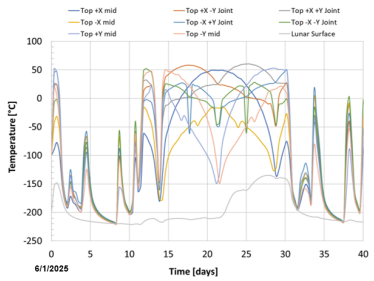

Top of Tower Temperature

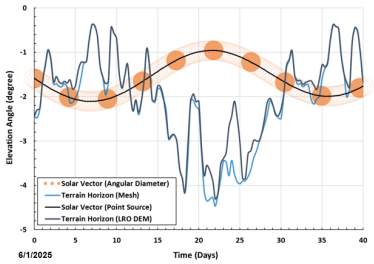

Terrain Horizon and Solar Path

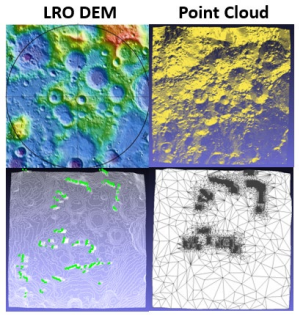

Tall Tower Lunar Thermal Analysis, Will Grier (LaRC-D206)[5]

Lunar Thermal Modeling Capability

- The current version of the HLS Lunar Thermal Analysis Guidebook and associated NESC Academy tutorial videos provide guidance on developing simplified and mission site specific Lunar surface thermal models[1][6]:
  - HLS-UG-001 Lunar Thermal Analysis Guidebook Baseline_STI.pdf
  - Lunar Thermal Analysis Guidebook, Part 1 | NESC Academy Online
  - Lunar Thermal Analysis Guidebook, Part 2 | NESC Academy Online
  - Lunar Thermal Analysis Guidebook, Part 3 | NESC Academy Online

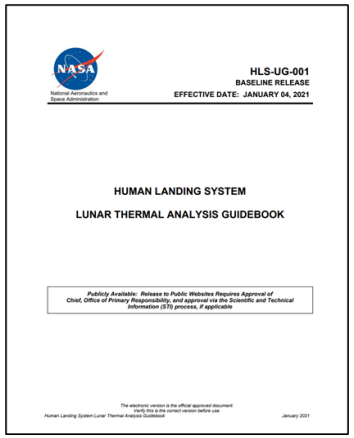

HLS-UG-001 Lunar Thermal Analysis Guidebook[1]

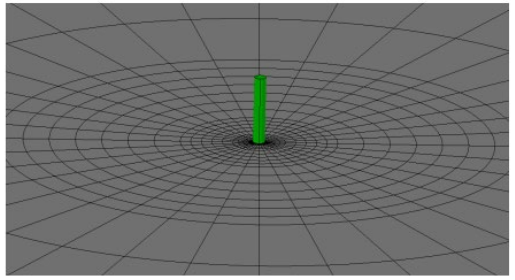

Simplified Flat Plane Surface Model[1]

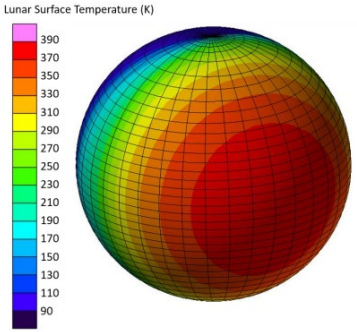

Lunar Surface Temperatures[1]

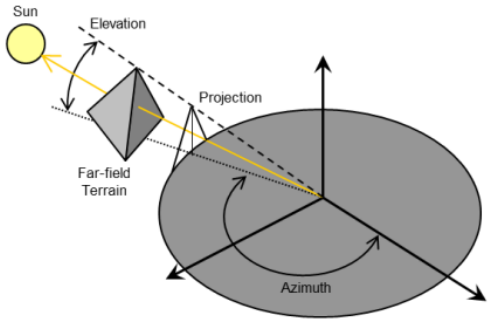

Far Field Terrain Impacts[1]

Detailed Site-Specific Terrain Mesh[1]

LUMENATE Detailed Terrain Thermal Model Updates

- Codifying a publicly releasable process to build Lunar thermal models that include site specific near-field terrain, far field terrain horizon, solar path, and regolith properties
  - Automated lunar surface point cloud simplification and generation (includes horizon points)
  - Process for obtaining solar vector and flux data for use in ANSYS Thermal Desktop (TD)
  - Verify surface temperature and illumination vs satellite data and detailed illumination models
- Lays groundwork for Lunar surface “weather reports” for Artemis EVA operations
  - Captures shadows and hot spots generated from detailed terrain features and surface assets
  - Used to predict suit temperatures to assist with EVA traverse planning
    - Identification of thermal keep out zones and EVA start and end times
    - Accurate temperature timeline prediction

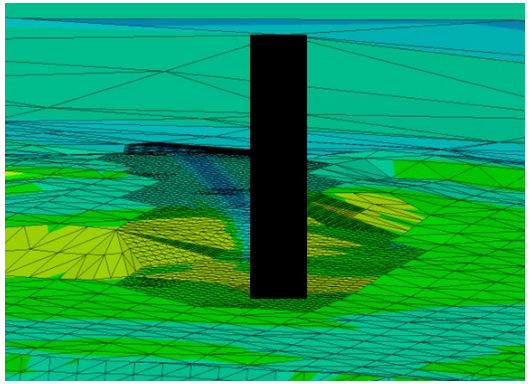

Lander Shadow on Lunar Surface (side view)

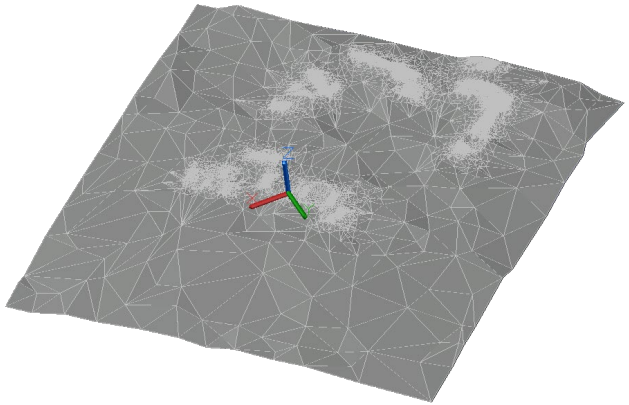

Manually Meshed Lunar Terrain with Horizon[5]

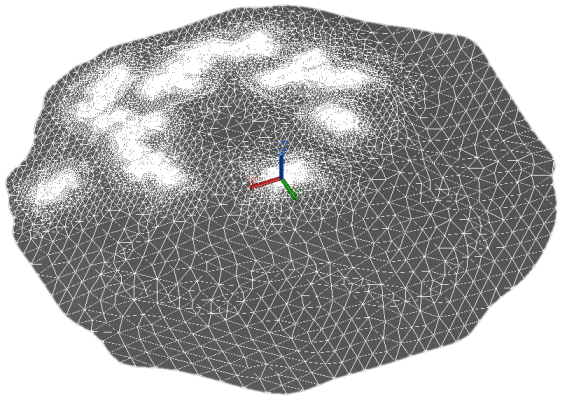

Automated Lunar Terrain Mesh with Horizon

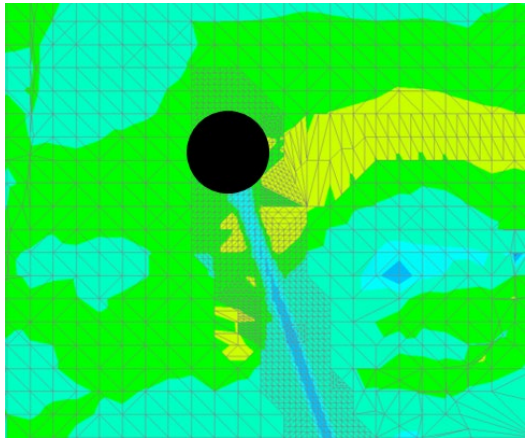

Lander Shadow on Lunar Surface (top view)

Lunar Surface Thermal Environment

The Lunar surface thermal environment is complex and significantly more extreme than Earth's in both magnitude and variation due to the following characteristics[1]:

- Regolith thermophysical and optical properties
  - Low thermal inertia, high IR emissivity, high solar absorptivity
- Lack of an atmosphere
  - Radiation dominant heat exchange, unobstructed incident solar flux
- Rotational period
  - ~29 Earth days with ~14.5-day nighttime duration
- Axial tilt to the ecliptic plane
  - 1.54º, complex solar illumination environment at the poles
- Complex and location dependent topology
  - Deep craters and high peaks

Accurately identifying worst case thermal environments for assets on the Lunar surface requires knowledge of the specific mission location:

- Maximum incident solar elevation angle
  - Latitude and local ground slope dependent
- View factor to surface
  - Nearby terrain topology, vehicle integration, height above surface
- Regional regolith thermophysical and optical properties

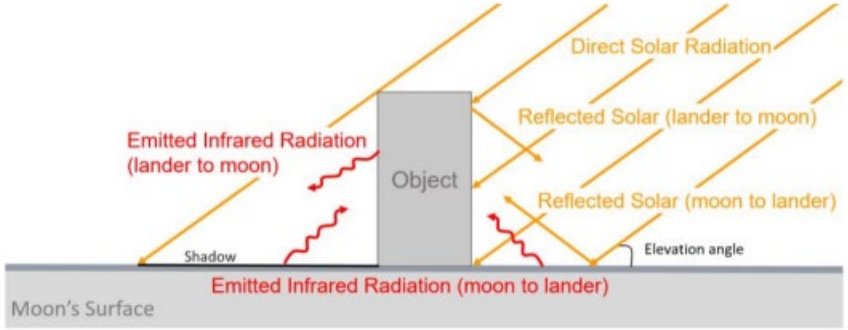

Radiation Exchange on Lunar Surface[1]

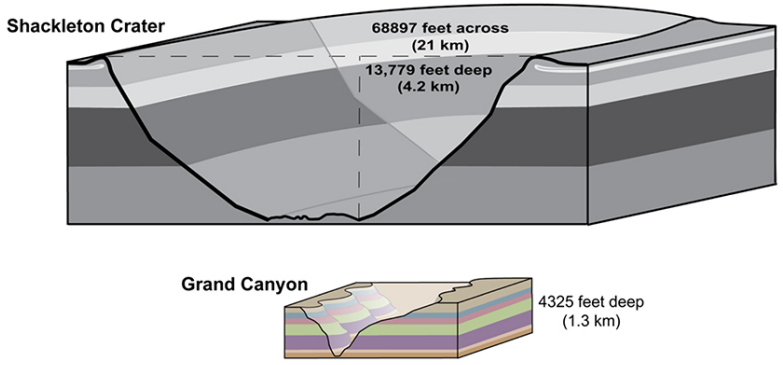

Shackleton Crater vs Grand Canyon[7]

Environmental Sink Temperature

Definitions:

- **Environmental Sink Temperature:** The effective temperature of the surrounding environment that acts as a thermal sink for radiative heat transfer from a surface. Represents a complex radiation environment as a single equivalent temperature.[8]
- **α/ε Ratio (Alpha-to-Epsilon Ratio):** The ratio of solar absorptivity to infrared emissivity. A low α/ε ratio surface absorbs little solar energy and emits most absorbed heat. A high α/ε ratio indicates high solar absorption with poor IR heat rejection capability.

Process:

- Flux cube optical properties are set to α_s=1 & ε_{IR}=1 in the Thermal Desktop (TD) model[11]
- Incident solar flux and TSINK are obtained via TD.hra files and the TSINK post processing routine respectively
- Incident IR flux is then back calculated using the formulas below
- Incident solar and IR fluxes can then be used with any optical property ratio to obtain the flux cube sink temperature

Thermal Radiation Exchange, Lunar Surface

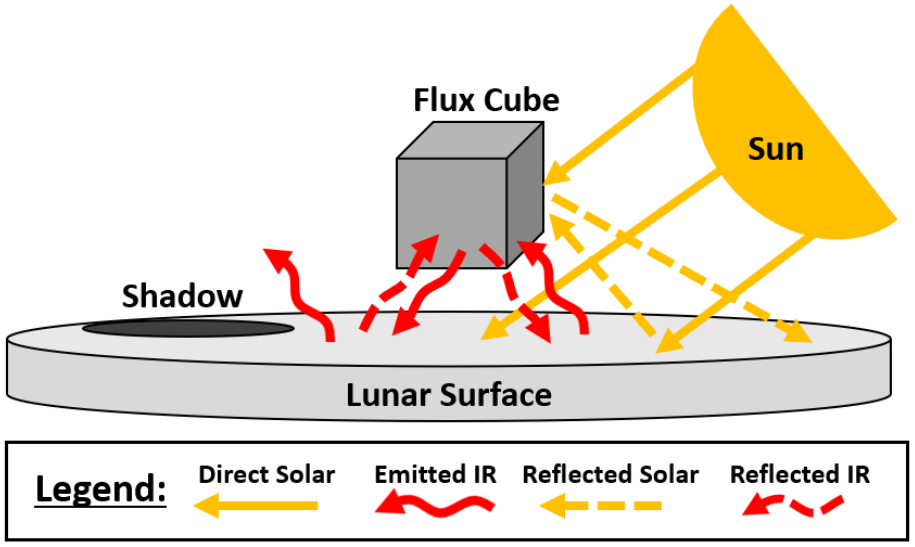

Environmental Sink Temperature Calculation[9,10]

$$0 = \alpha_s Q_s + \varepsilon_{IR} Q_{IR} - \varepsilon_{IR} \sigma T_\infty^4$$

$$T_\infty = \left(\frac{1}{\sigma} \left(\frac{\alpha_s}{\varepsilon_{IR}} Q_s + Q_{IR} \right) \right)^{0.25}$$

$$Q_s = \frac{\varepsilon_{IR}}{\alpha_s} (\sigma T_\infty^4 - Q_{IR})$$

$$Q_{IR} = (\sigma T_\infty^4 - \frac{\alpha_s}{\varepsilon_{IR}} Q_S)$$

Parameter	Symbol	Unit
Solar Absorptivity	α_s	N/A
Absorbed Solar Flux	Q_s	W/m²
IR Emissivity	ε_{IR}	N/A
Absorbed IR Flux	Q_{IR}	W/m²
Environmental Sink Temperature	T_∞	K
Stefan-Boltzmann Constant	σ	W/m²K⁴

Simple Ground Plane Model Overview & Assumptions

- **Used Thermal Desktop to analyze the environmental sink temperatures of a Flux Cube in Lunar polar, mid-latitude, and equatorial locations**
  - Simplified flat ground plane with radius of 150m representing the Lunar surface
  - Investigated date range: 1/1/2028 to 1/1/2029
  - Flux cube modeled as 0.1x0.1x0.1m arithmetic node cube
    - No internal heat generation
    - Uniform surface optical properties
  - Flux cube is separated from ground plane by 2m

Analyzed Locations

Location	Latitude	Longitude
Polar	-89.46752°	-138.012788°
Mid-Latitude	+45°	0°
Equatorial	0°	0°

- **Lunar environment defined using LTAG, Design Specification for Natural Environments (DSNE), and JPL Horizons data [1][12,13]**
  - Subsurface layer temperatures initialized (cyclic steady state) via transient model run (2009 to 2028)[1]
  - Time varying and location dependent solar vector path and solar flux from JPL Horizons[13]
  - Surface IR emissivity[14] and solar absorptivity[15,16] (incident angle dependent)
    - highland directional α_s (polar)[16] and mare directional α_s (mid-latitude & equatorial)[15]
  - Surface density[17,18] and specific heat[19] (depth dependent)
  - Surface thermal conductivity (depth and temperature dependent) [18]
  - Solar diameter (subtended) angle (0.53°)[1]
  - Subsurface ground heat flow (~0.018 W/m²)[20]
  - Impacts from regolith dust deposition can be inferred via optical property ratio[1]

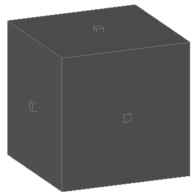

Arithmetic Node Flux Cube

- **Not included in thermal model**
  - Site specific terrain (local slope, adjacent hills, horizon, craters, boulders)
  - Vehicle geometry or occlusion (lander, platform, etc.)
  - Earthshine (0 to 0.15 W/m²) and eclipses (~hours)[1]

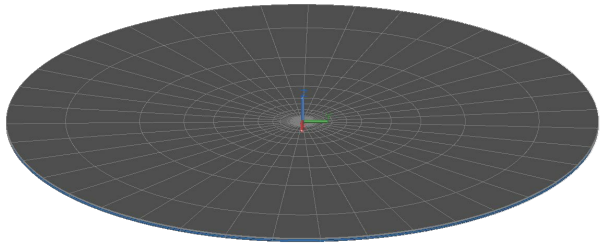

Flat Ground Plane, Lunar Surface

Location: South Pole (89.5ºS)

- At the poles, the solar elevation angle remains low with the sun circling close to the horizon; This creates a low solar incident angle relative to the terrain, resulting in relatively cool ground temperatures despite direct sunlight
- The flux cube's side faces receive solar illumination, the bottom face receives some IR and reflected solar heat from the lunar surface, and the top face predominantly radiates to deep space with minimal solar input

Solar Absorptivity (α_s)	IR Emissivity (ε_{IR})	Ratio ($\alpha_s/\varepsilon_{IR}$)
0.1	0.9	0.1
0.35	0.7	0.5
0.5	0.5	1
0.7	0.35	2

Solar Elevation Angle & Flux vs Time

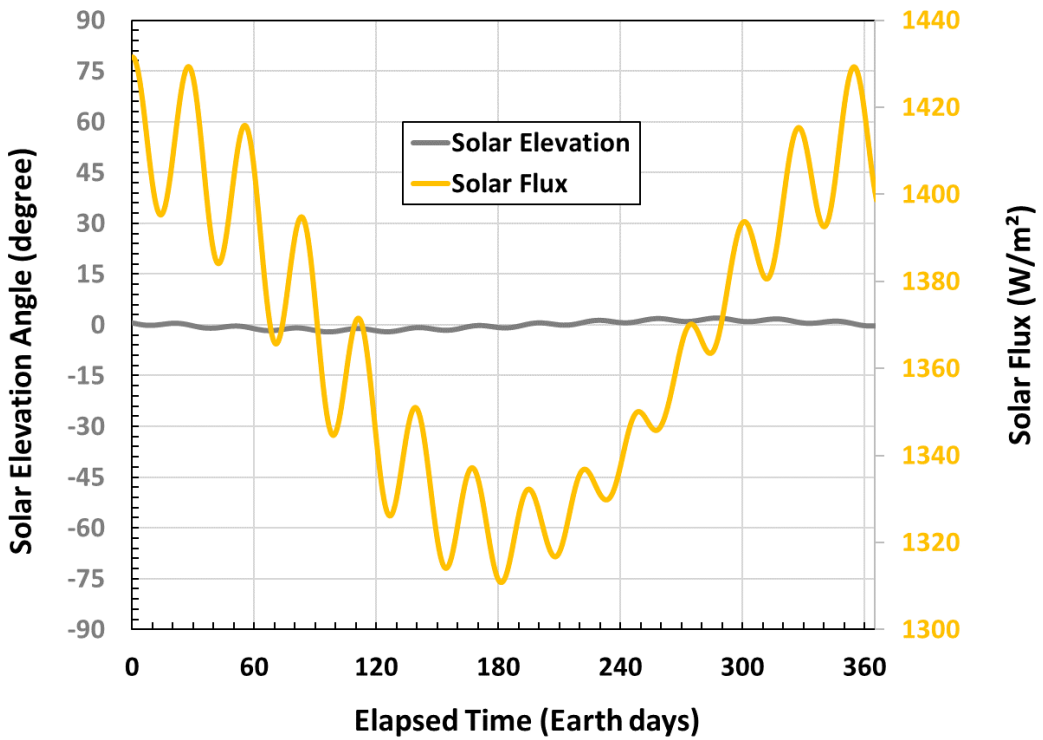

Sink Temperature vs α/ε Ratio

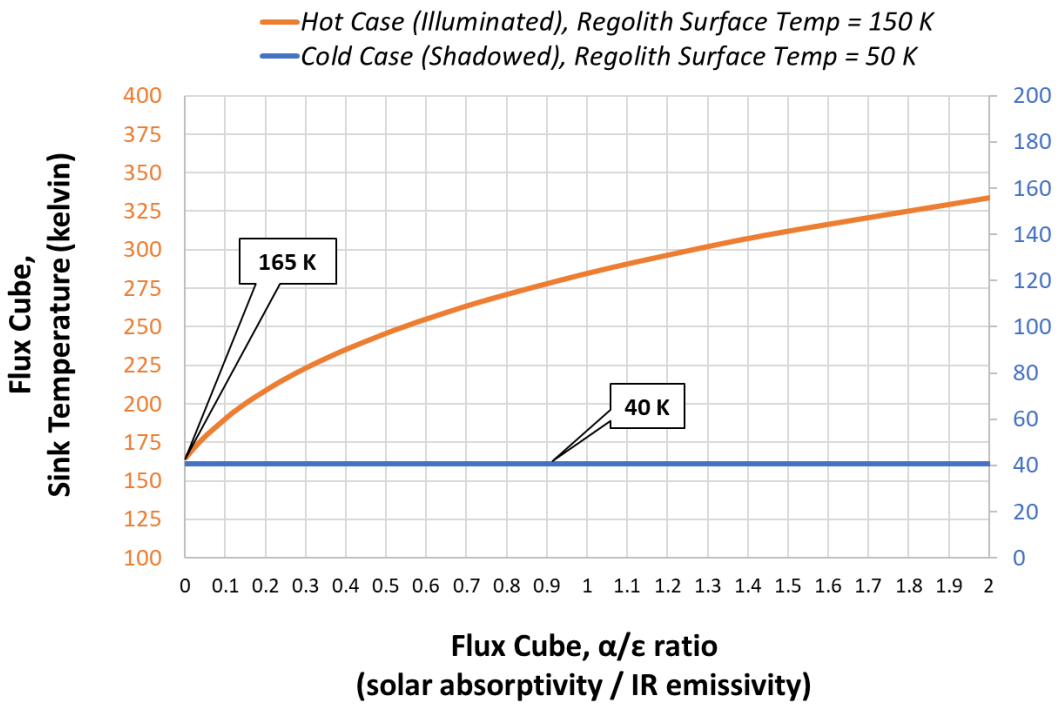

Note: Environmental sink temperature vs. optical property ratio trends were derived from analysis timesteps selected based on peak sink temperatures (hot and cold)

Location: Mid-Latitude (45ºN)

- At mid-latitudes, the solar elevation angle varies throughout the day with the sun arcing higher across the sky than at the poles generating relatively higher surface temperatures
- The flux cube's side faces receive alternating periods of direct and indirect solar illumination, the bottom face receives heat from a hotter Lunar surface, and the top face periodically receives indirect sunlight

Solar Absorptivity (α_s)	IR Emissivity (ε_{IR})	Ratio ($\alpha_s/\varepsilon_{IR}$)
0.1	0.9	0.1
0.35	0.7	0.5
0.5	0.5	1
0.7	0.35	2

Solar Elevation Angle & Flux vs Time

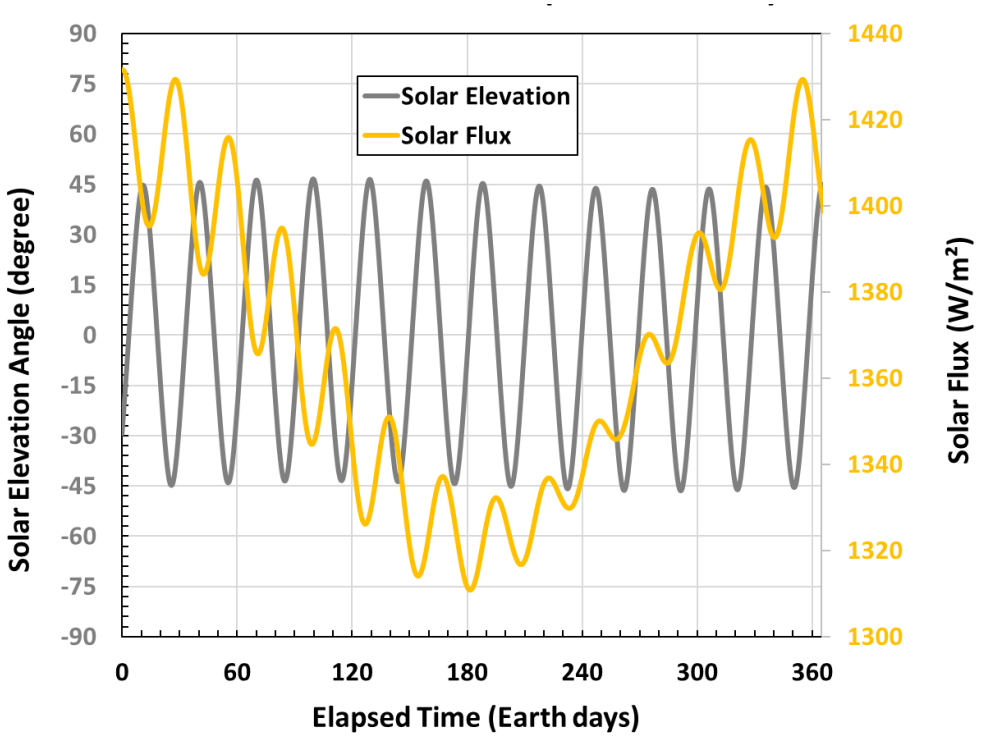

Sink Temperature vs α/ε Ratio

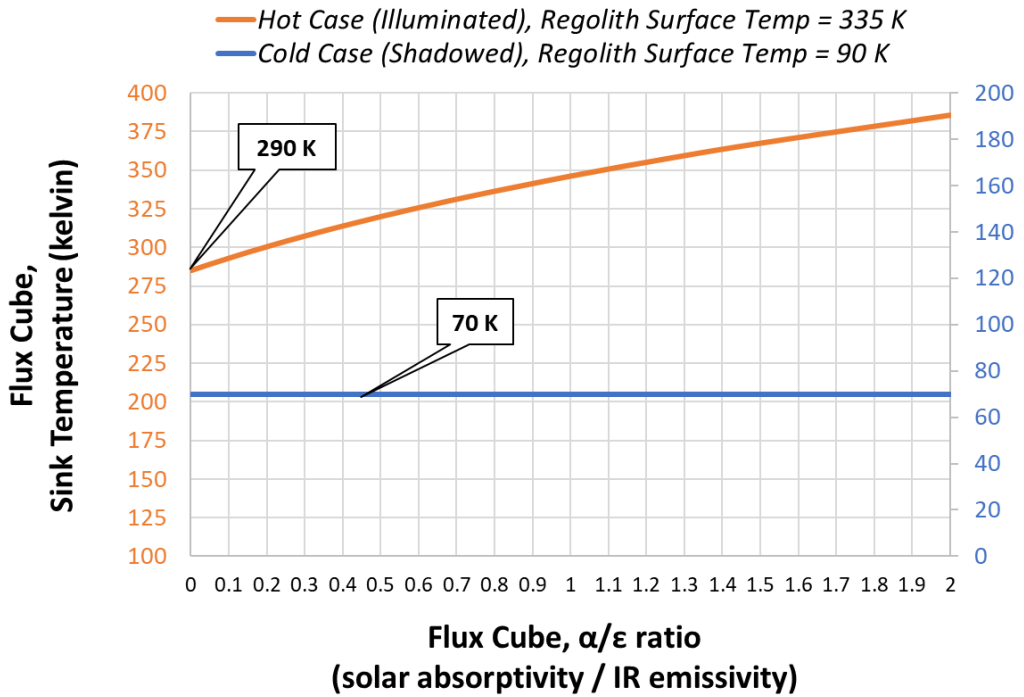

Note: Environmental sink temperature vs. optical property ratio trends were derived from analysis timesteps selected based on peak sink temperatures (hot and cold)

Location: Equatorial (0ºN)

- At the lunar equator, the solar path reaches zenith during local noon with near-perpendicular solar incident angles relative to the terrain thus generating high Lunar surface temperatures
- The flux cube's side faces receive directional solar illumination as the sun moves overhead, the bottom face exchanges heat with a surface that reaches high peak temperatures, and the top face receives maximum solar input during lunar noon

Solar Absorptivity (α_s)	IR Emissivity (ε_{IR})	Ratio ($\alpha_s/\varepsilon_{IR}$)
0.1	0.9	0.1
0.35	0.7	0.5
0.5	0.5	1
0.7	0.35	2

Solar Elevation Angle & Flux vs Time

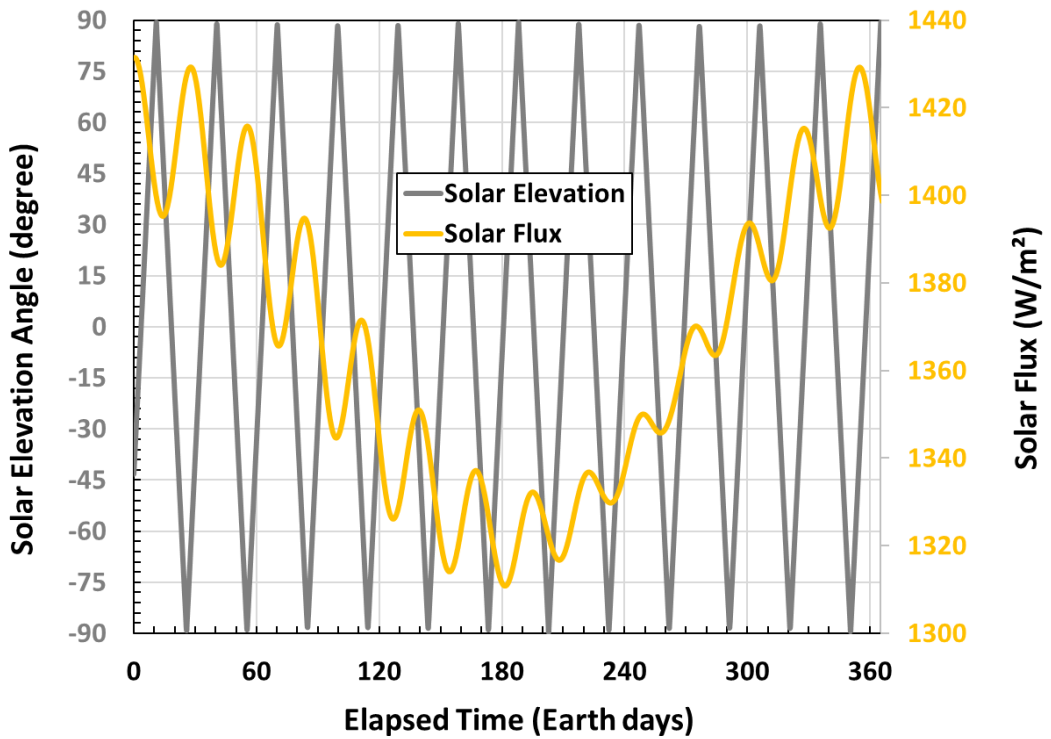

Sink Temperature vs α/ε Ratio

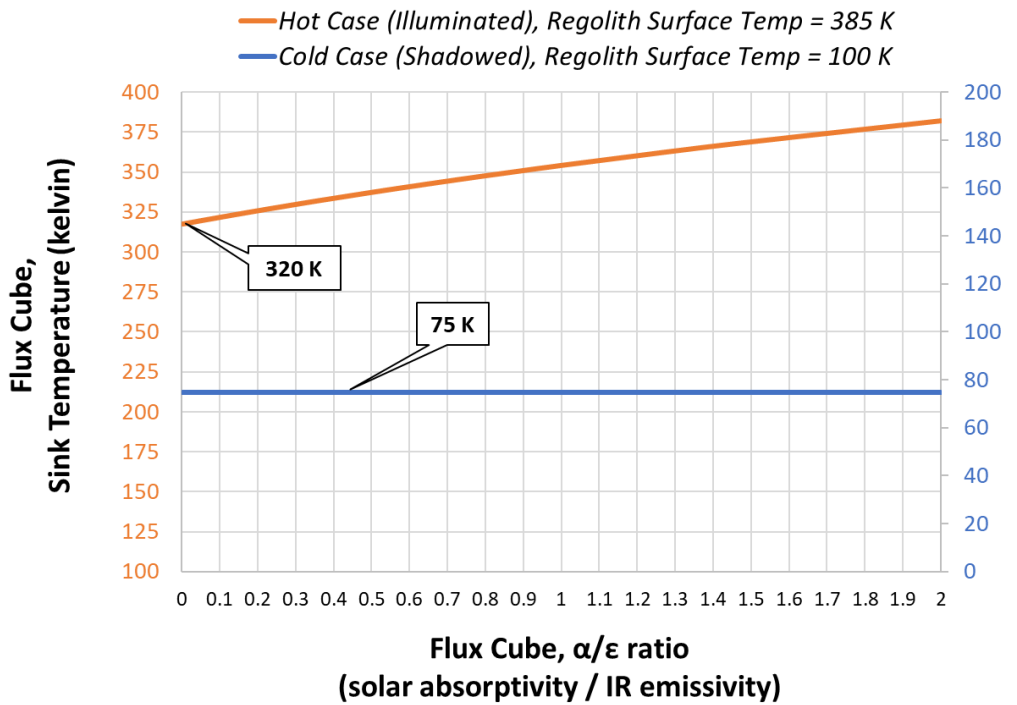

Note: Environmental sink temperature vs. optical property ratio trends were derived from analysis timesteps selected based on peak sink temperatures (hot and cold)

Results: Flat Ground Plane

- Sink temperature is almost never equivalent to regolith surface temperature
  - Hot case (illuminated, daytime); equatorial = hottest region:
    - Sink temperature increases (↑) with decreasing (↓) latitude
  - Cold case (shadowed, nighttime); polar = coldest region
    - Sink temperature decreases (↓) with increasing (↑) latitude

Polar, Hot Case, Regolith Surface Temp = 150 K
Mid-Latitude, Hot Case, Regolith Surface Temp = 335 K
Equatorial, Hot Case, Regolith Surface Temp = 385 K
Polar, Cold Case, Regolith Surface Temp = 50 K
Mid-Latitude, Cold Case, Regolith Surface Temp = 90 K
Equatorial, Cold Case, Regolith Surface Temp = 100 K

Flat Ground Plane, Regional Sink Temperature vs α/ε Ratio

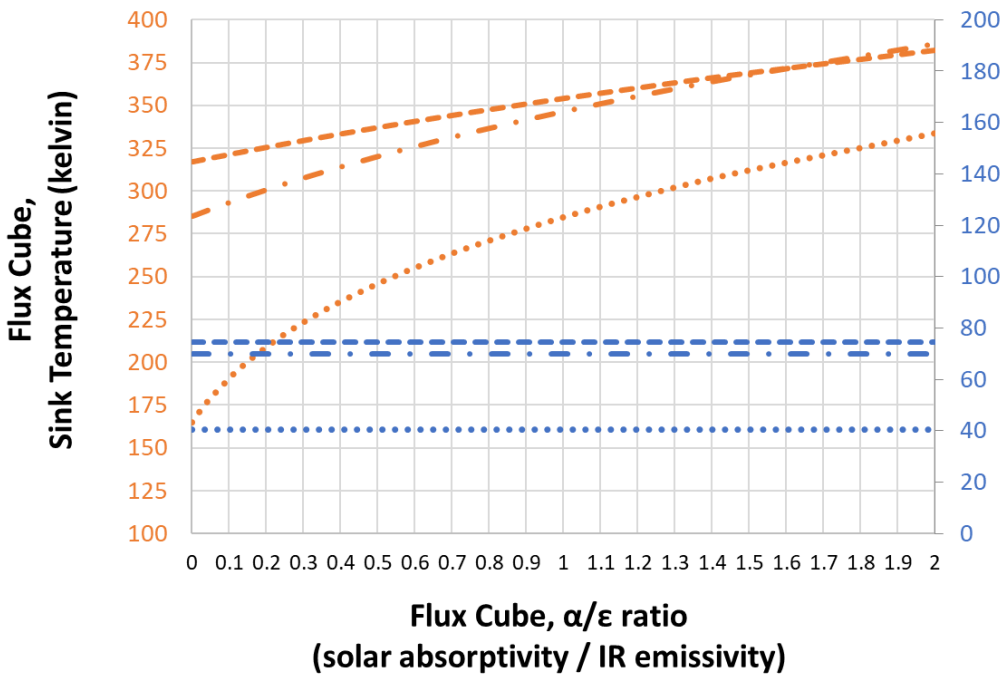

Flat Ground Plane, Regional ΔT vs α/ε Ratio

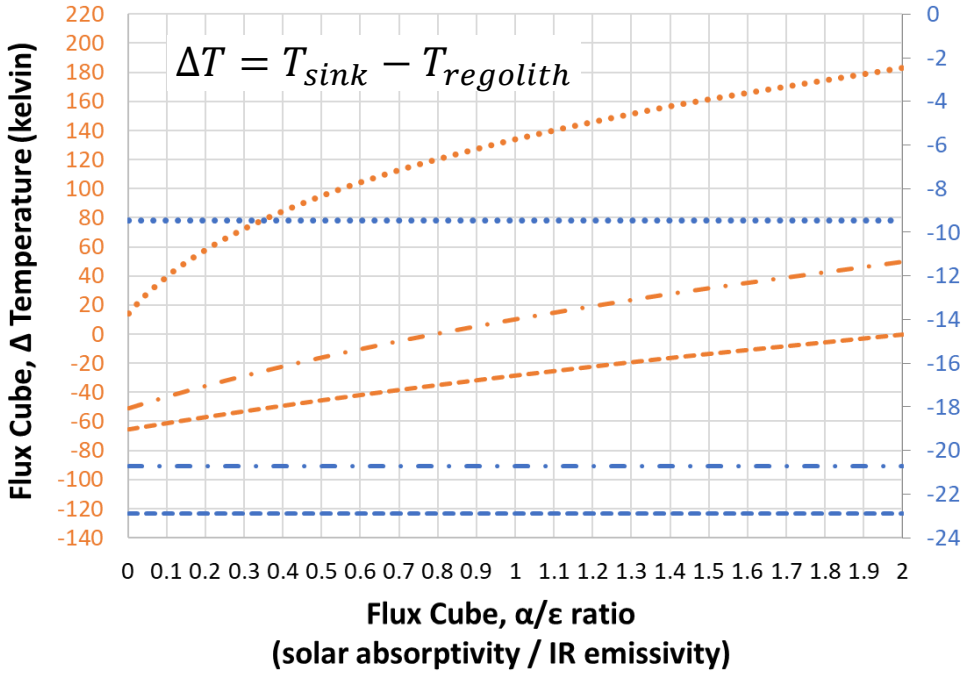

Note: Environmental sink temperature vs. optical property ratio trends were derived from analysis timesteps selected based on peak sink temperatures (hot and cold)

Detailed Terrain Model Overview & Assumptions

- **Used Thermal Desktop to analyze environmental sink temperatures of a Flux Cube at the Shackleton Connecting Ridge (latitude = -89.46752º, longitude = -138.012788º, elevation = 1938 m)**
  - Site specific surface terrain (including horizon) incorporated from previous thermal model[5]
  - Investigated date range: 1/1/2028 to 1/1/2029
  - Flux cube modeled as 0.1x0.1x0.1m arithmetic node cube
    - No internal heat generation
    - Cube has uniform optical properties
  - Flux cube is separated from Lunar surface by 2m
- **Lunar environment defined using LTAG, DSNE, and JPL Horizons data [1][12,13]**
  - Includes site specific terrain (local slope, adjacent hills, craters, and horizon)
  - Subsurface layer temperatures initialized (cyclic steady state) via transient model run (2009 to 2028)[1]
  - Time varying and location dependent solar vector path and solar flux from JPL Horizons[13]
  - Surface IR emissivity[14] and solar absorptivity[15,16] (incident angle dependent)
    - highland directional α_s (polar)[16]
  - Surface density[17,18] and specific heat[19] (depth dependent)
  - Surface thermal conductivity (depth and temperature dependent) [18]
  - Solar diameter (subtended) angle (0.53º)[1]
  - Subsurface ground heat flow (~0.018 W/m²)[20]
  - Impacts from regolith dust deposition can be inferred via optical property ratio[1]
- **Not included in thermal model**
  - Vehicle geometry or occlusion (lander, platform, etc.)
  - Earthshine (0 to 0.15 W/m²) and eclipses (~hours)[1]

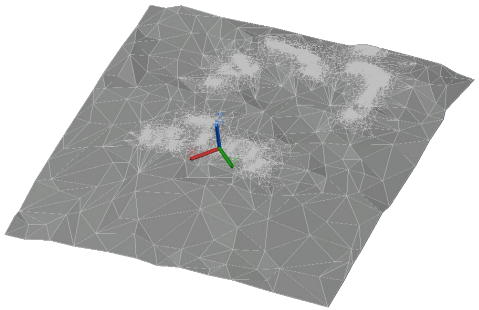

Manually Generated Detailed Terrain Mesh[5]

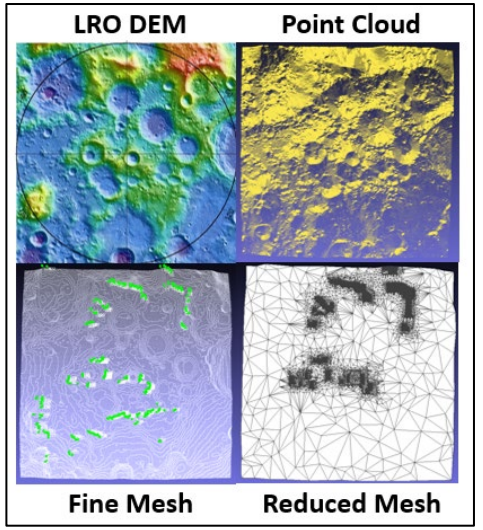

Site Terrain Generation Process[5]

Comparison: Polar, Simplified vs Detailed Surface Model

- Sink temperature curves differ between detailed terrain and simple flat plane models (with stated assumptions)
  - Difference magnitude can vary widely depending on surface site of interest and asset vehicle integration and orientation
- Sink temperature is still almost never equivalent to regolith surface temperature

Flat Ground Plane Model

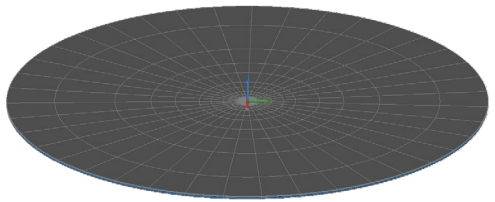

Detailed Terrain Model[5]

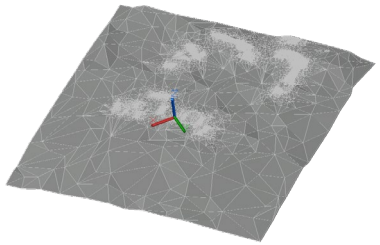

Sink Temperature vs α/ε Ratio & Terrain Model

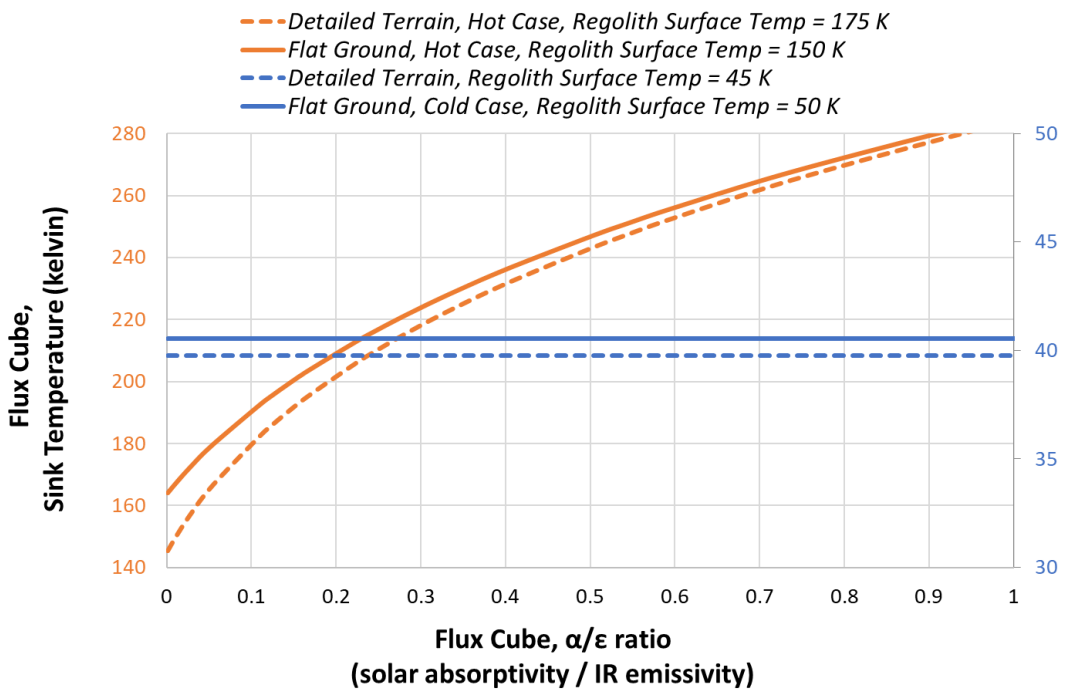

Δ Sink Temperature vs α/ε Ratio & Terrain Model

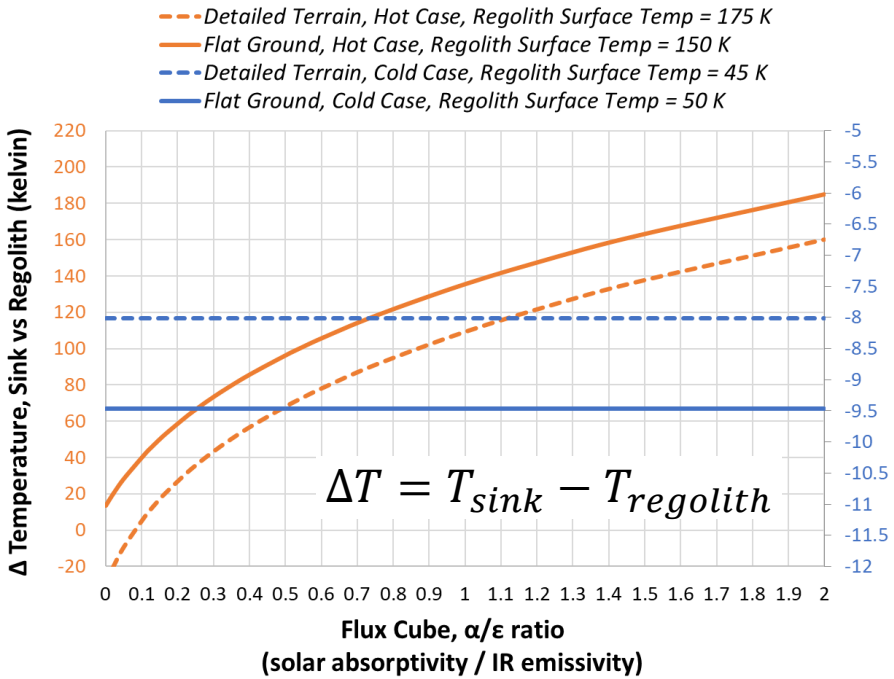

Note: Environmental sink temperature vs. optical property ratio trends were derived from analysis timesteps selected based on peak sink temperatures (hot and cold)

Accounting for Lunar Dust Impacts

- Regolith dust deposition onto asset surfaces can be inferred by applying optical property ratio factors that are derived from experimental test data
  - Factors correspond to percent dust coverage for different surface treatments and regional regolith compositions
- Dust deposition effectively increases the sink temperature thus limiting heat rejection capability which may result in higher temperatures during the day and longer nighttime survival durations
  - See Will Birmingham's *"Lunar South Pole Terrain Effects on Radiators"* paper for a more detailed analysis on the thermal effects of terrain and dust deposition for radiators

Dusted Surface Optical Property Factors

Optical Property	Solar Absorptivity (α_s)	IR Emissivity (ε_{IR})	Ratio ($\alpha_s/\varepsilon_{IR}$)	$\frac{(\alpha_s/\varepsilon_{IR})_{dusted}}{(\alpha_s/\varepsilon_{IR})_{pristine}}$	Detailed Terrain, Sink Temp (K)
Baseline	0.15	0.85	0.18	1.0	200
Degraded	0.20	0.80	0.25	1.4	213
	0.25	0.75	0.33	1.9	225
	0.30	0.70	0.43	2.4	237
	0.35	0.65	0.54	3.1	248

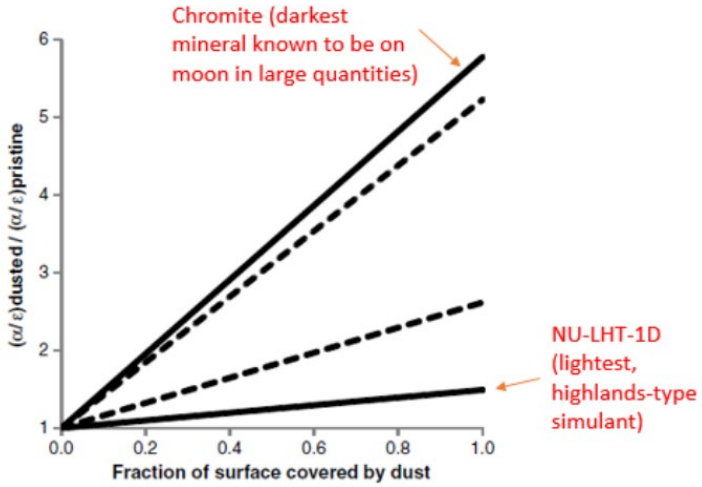

Varying Optical Properties of Typical Radiator Materials vs Dust Deposition for Regional Simulants[1]

Polar, Sink Temperature vs α/ε Ratio

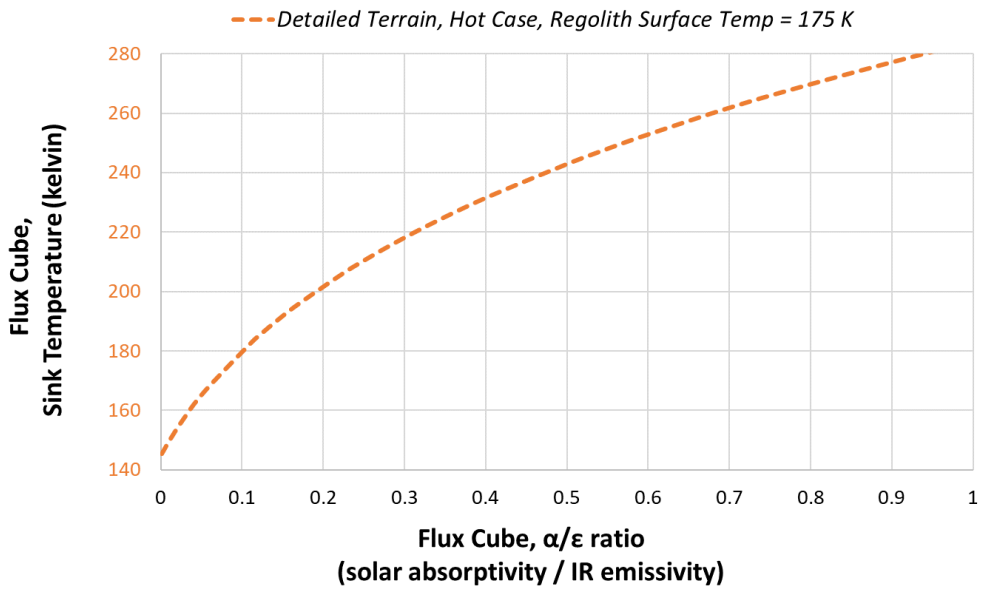

Method Comparison: Predicting Surface Temperature

- For polar locations, flat ground plane models do not accurately capture worst case hot environment due to the relationship between local terrain slope, solar elevation angle, and incident angle regolith optical properties
  - 240 meters per pixel resolution of LRO satellite derived bolometric surface temperature data limits its utility for areas of extreme topology
- For mid-latitude and equatorial regions, a flat ground plane model will capture worst case hot and cold conditions within 7 K (assuming the site of interest is relatively flat)

Lunar Location	Terrain Model Type	Latitude	Longitude	Maximum Regolith Surface Temperature (kelvin)					Minimum Regolith Surface Temperature (kelvin)			
				Model Predicted	DSNE Regional Mean[12]	DSNE Regional 1σ[12]	**LTAG Section 5.2.2[1]	***LRO Data @ Lat, Long	Model Predicted	DSNE Regional Mean[12]	DSNE Regional 1σ[12]	***LRO Data @ Lat, Long
Polar	*Ground Plane*	-89.46752°	-138.012788°	**160**	*182 (@ 85°S)	*224 (@ 85°S)	119	237	**50**	*61 (@ 85°S)	*41 (@ 85°S)	63
Polar	*Detailed Terrain*	-89.46752°	-138.012788°	**185**					**47**			
Mid-Latitude	*Ground Plane*	+45°	0°	**354**	350	357	359	355	**91**	89	83	93
Equatorial	*Ground Plane*	0°	0°	**387**	391	394	392	394	**98**	96	94	99

*Polar mean and 1σ worst case hot and cold values as listed in DSNE; originally obtained via LRO Diviner flight data for 85º Latitude locations

**For mid-latitude and equatorial locations, daytime surface temperatures can be approximated via analytical expressions based on an energy balance

***Values were obtained via LROC WebView, LRO Diviner data was overlayed onto a digital elevation map of the Lunar surface. LRO Diviner bolometric Lunar surface temperature data has a spatial resolution of 240 meters per pixel and temperature value error of ±5ºC. For polar regions where terrain topology is extreme and the solar vector stays near the horizon, the relatively low spatial data resolution of the Diviner instrument can reduce its utility for estimating surface temperatures.[21-25]

LRO Data @ Lat, Long:

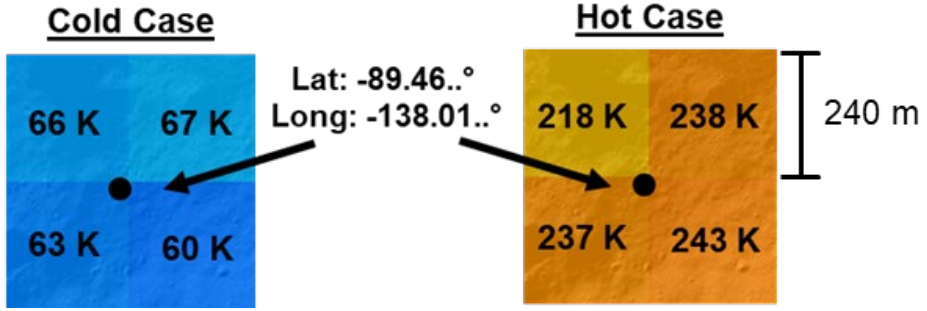

Findings and Remarks

- Regolith surface temperatures are not the effective thermal environment that assets near or on the surface will experience, asset sink temperature is almost never equivalent to regolith surface temperature
  - Accurately identifying the worst-case thermal environments for assets on the Lunar surface requires knowledge of the specific mission location (terrain features, regolith properties, solar elevation angle) and vehicle integration (e.g., reflections or occlusion from the environment)
  - Asset temperatures can be much hotter or colder than Lunar surface temperatures

- For polar locations, flat ground plane models do not accurately capture worst case hot surface temperature due to the relationship between local terrain slope, solar elevation angle, and incident angle regolith optical properties
  - 240 meters per pixel resolution of LRO satellite derived bolometric surface temperature data limits its accuracy for areas of extreme topology

- For mid-latitude and equatorial regions, a flat ground plane model can capture worst case hot and cold surface temperatures within ±7 K (assuming the site of interest is relatively flat)

- The thermal impacts of regolith dust deposition onto asset surfaces can be inferred by applying optical property ratio factors that are derived from experimental test data
  - Factors correspond to percent dust coverage for different surface treatments and regional regolith compositions

References

[1] B. D. Hamill, R. G. Schunk, and L. R. Erickson, “Human Landing System Lunar Thermal Analysis Guidebook,” Jan. 2021, Available: https://ntrs.nasa.gov/citations/20210010030

[2] C. Gomez, B. Hamill, G. Schunk, and L. Erickson, “Lunar Surface 3D Terrain Modeling,” Sep. 06, 2022. Available: https://ntrs.nasa.gov/citations/20220013302

[3] W. Birmingham, “Thermal Sensitivity Study of Lunar Terrain Vehicle Wheels.” Accessed: Jun. 12, 2025. [Online]. Available: https://ntrs.nasa.gov/api/citations/20240006096/downloads/Thermal%20Sensitivity%20of%20LTV%20Wheels%20V4.pdf

[4] W. Birmingham, G. Schunk, and B. Evans, “Lunar Latitude and Terrain Radiator Sensitivity Study,” 2024. [Online]. Available: https://ntrs.nasa.gov/api/citations/20240010276/downloads/Lunar_Latitude_and_Terrain_Radiator_Sensitivity_V2.pdf

[5] W. Grier, A. Stark, R. Wiggins, and R. Amundsen, “Thermoplastic Space Point Design (TSPD) Tall Tower Lunar Thermal Analysis,” Nasa.gov, Aug. 26, 2024. https://ntrs.nasa.gov/citations/20240009936

[6] “Lunar Thermal Analysis Guidebook, Part 1,2,3 | NESC Academy Online,” nescacademy.nasa.gov. https://nescacademy.nasa.gov/video/43723e634fe44646aef30b745640ad4d1d

[7] “Lunar Surface Geology,” Usra.edu, 2025. https://www.lpi.usra.edu/exploration/training/illustrations/lunarGeology/ (accessed Jun. 12, 2025).

[8] A. Juhasz, “An Analysis and Procedure for Determining Space Environmental Sink Temperatures With Selected Computational Results,” 2001. Available: https://ntrs.nasa.gov/api/citations/20010014168/downloads/20010014168.pdf

[9] L. Carrillo, N. Jsc, D. Farner, J. Engineering, and C. Preston, “NASA-TFAWS Short Course ISS Payload Thermal Environments,” 2015. Accessed: Jul. 01, 2025. [Online]. Available: https://tfaws.nasa.gov/wp-content/uploads/TFAWS2015-SC-ISS-Payload-Thermal-Design.pdf

[10] L. Erickson, B. Barnes, C. Sladek, “Thermal Analysis for EVA Twighlight Scenario on a Flat Plane,” JETS-JE33-23-TLSS-DOC-00031, June 8, 2023.

[11] R. Henson, G. Laubach, J. Iovine, G. Lucas, “A Routine (FLXCAL) to Determine EVA Cube Fluxes using SINDA Temperatures,” June 20, 2003.

[12] F. B. Leahy, “SLS-SPEC-159, Cross-Program Design Specification for Natural Environments (DSNE),” Oct. 2021. Available: https://ntrs.nasa.gov/citations/20210024522

[13] “Horizons System,” Available: https://ssd.jpl.nasa.gov/horizons/

[14]T.-Y. Park, J.-J. Lee, J.-H. Kim, and H.-U. Oh, “Preliminary Thermal Design and Analysis of Lunar Lander for Night Survival,” International Journal of Aerospace Engineering, vol. 2018, pp. 1–13, Oct. 2018, doi: https://doi.org/10.1155/2018/4236396.

[15] J. Feng, M. A. Siegler, and P. O. Hayne, “New Constraints on Thermal and Dielectric Properties of Lunar Regolith from LRO Diviner and CE-2 Microwave Radiometer,” Journal of Geophysical Research: Planets, vol. 125, no. 1, Jan. 2020, doi: https://doi.org/10.1029/2019je006130

[16] E. J. Foote, D. A. Paige, M. K. Shepard, J. R. Johnson, and S. Biggar, “The bidirectional and directional hemispheric reflectance of Apollo 11 and 16 soils: Laboratory and Diviner measurements,” Icarus, vol. 336, p. 113456, Jan. 2020, doi: 10.1016/j.icarus.2019.113456.

[17] A. R. Vasavada et al., “Lunar equatorial surface temperatures and regolith properties from the Diviner Lunar Radiometer Experiment,” Journal of Geophysical Research: Planets, vol. 117, no. E12, p. n/a-n/a, Apr. 2012, doi: https://doi.org/10.1029/2011je003987.

[18] P. O. Hayne et al., “Global Regolith Thermophysical Properties of the Moon From the Diviner Lunar Radiometer Experiment,” Journal of Geophysical Research: Planets, vol. 122, no. 12, pp. 2371–2400, Dec. 2017, doi: https://doi.org/10.1002/2017je005387.

[19] R. Woods-Robinson, M. A. Siegler, and D. A. Paige, “A Model for the Thermophysical Properties of Lunar Regolith at Low Temperatures,” Journal of Geophysical Research: Planets, vol. 124, no. 7, pp. 1989–2011, Jul. 2019, doi: https://doi.org/10.1029/2019je005955

[20] L. Erickson, C. Gomez, B. Hamill, and G. Schunk, “Lunar Thermal Analysis Guidebook: Thermo-physical and Optical Properties of Lunar Regolith.” Available: https://ntrs.nasa.gov/api/citations/20220013412

[21] “Lunar Reconnaissance Orbiter - NASA Science,” Available: https://science.nasa.gov/mission/lro/

[22] “Lunar Orbital Data Explorer - Data Set Browser,” ode.rsl.wustl.edu. https://ode.rsl.wustl.edu/moon/datasets

[23] “QuickMap,” quickmap.lroc.asu.edu. Available: https://quickmap.lroc.asu.edu

[24] T. M. Powell et al., “High-Resolution Nighttime Temperature and Rock Abundance Mapping of the Moon Using the Diviner Lunar Radiometer Experiment With a Model for Topographic Removal,” Journal Of Geophysical Research: Planets, vol. 128, no. 2, Feb. 2023, doi: https://doi.org/10.1029/2022je007532.

[25] J. P. Williams et al., “Seasonal Polar Temperatures on the Moon,” JGR Planets, vol. 124, no. 10, pp. 2505–2521, Oct. 2019, doi: https://doi.org/10.1029/2019je006028.